

Production by 3D printing of modular tools for highly customizable hydroforming of light sheet metals

Pasquale Guglielmi^{1,a*}, Antonio Piccininni^{2,b}, Paola Ginestra^{3,c}, Angela Cusanno^{2,d}, Andrea Abeni^{3,e}, Valerio Minafra^{2,f}, Elisabetta Ceretti^{3,g}, Gianfranco Palumbo^{2,h}

¹Dept. of Engineering, University of Basilicata, Via Ateneo Lucano 10, Potenza, 85100, Italy

²Dept. of Mechanics, Mathematics and Management, Politecnico di Bari, Via Orabona 4, 70125 Bari, Italy

³Dept. of Mechanical and Industrial Engineering, University of Brescia, Via Branze 38, 25123 Brescia, Italy

^apasquale.guglielmi@unibas.it, ^bantonio.piccininni@poliba.it, ^cpaola.ginestra@unibs.it, ^dangela.cusanno@poliba.it, ^eandrea.abeni@unibs.it, ^fv.minafra1@studenti.poliba.it, ^gelisabetta.ceretti@unibs.it, ^hgianfranco.palumbo@poliba.it

Keywords: HydroForming, FE Model, Modular Tool

Abstract. The present work proposes an innovative approach for producing complex shaped parts by HydroForming (HF) based on the adoption of customizable and modular polymeric dies fabricated via 3D printing. The proposed approach was tested on a benchmark axisymmetric Aluminum (Al) alloy component (AA5754-H111, initial thickness: 0.5 mm) with undercuts. The HF process was conducted at room temperature; the commercial Finite Element (FE) code Abaqus/CAE was used to define the oil pressure profile and the load applied by the blankholder to successfully fill the die cavity. In addition, the FE model allowed to study the effect of the assembly configuration of the die's polymeric subparts in terms of shape and thickness of the component. The proposed approach provides an innovative tool that combines flexibility, adaptability, and precision for the manufacturing of complex shaped parts by HF.

Introduction

The demanding requirements imposed by the national and international regulations in terms of harmful emissions are underlining the importance of updating the design criteria toward a massive adoption of lighter structural components [1]. The transportation sector is a key contributor to emissions, and the automotive industry is constantly evolving, focusing on reducing vehicle weight to lower fuel consumption and emissions. Weight reduction can be achieved through various approaches, such as selecting lightweight materials, improving their production processes, and optimizing design. The most used new materials for such applications include (i) Advanced Steels, (ii) Polymers, (iii) Composites, (iv) Magnesium alloys and especially (v) Al alloys [2]. Al alloys are of particular interest in the automotive field due to their recyclability and excellent strength-to-weight ratio. They are typically used in the production of frames and body panels, offering a weight reduction up to 60% [3]. Al alloys represent a viable solution capable to combine strength and limited weight, even though the limited formability at room temperature still counterbalances the abovementioned advantages. To overcome such a limitation, innovative sheet metal forming processes using flexible media have gained visibility: the HF process, in which a pressurized oil forces the blank to fill the die cavity, possesses the capability to obtain complex shaped parts with enhanced mechanical properties, more uniform thickness, better surface finish and a near net-shape [4]. HF allows to better exploit the material formability than traditional cold forming, with lower costs and a relatively shorter cycle time than other advanced forming techniques able to produce complex shaped parts like superplastic forming or incremental forming. Such an enhanced

exploitation of the material formability is demonstrated by an increase in the Limit Drawing Ratio, from 2 in deep drawing to 3.2 in HF [5]. Additionally, HF offers advantages over conventional stamping, such as the capability to work with stronger materials, improve tolerances, repeatability, and dimensional accuracy, while reducing elastic springback and residual stresses. Despite technological advances and engineering improvements that enable large-scale production, there are still areas for improvement and unresolved issues. A limitation of the process, for example, is the high difficulty in obtaining components with undercuts, which could not be extracted from the metal die. In this sense, Flexform, also known as fluid cell forming, is a low-cost sheet metal forming process used for both prototyping and low-volume production. The Flexform process requires only one tool half and a draw ring, which is placed on the moving press table. The blank material is positioned on the tool half before the press table returns to its position. The forming process occurs by pressurizing the rubber membrane with a liquid, typically oil, which shapes the sheet metal to the desired geometry [6]. In general, for analysing the process, optimizing the design and production of formed parts, FE simulations are very useful. This is especially true when metal or complex dies (such as modular ones) need to be produced; indeed, this approach significantly reduces the risk of failure and, consequently, leads to a notable increase in cost savings.

The present work focused on a potential technological update of the HF process that involves the use of modular dies made of polymeric material using Additive Manufacturing (AM) technique. Additionally, modular dies enable rapid geometric modifications of the component without needing to redesign the hydroforming tooling, making the process more versatile. Aluminum AA5754-H111 sheets, a widely used alloy in the automotive sector, were used. The study was based on the numerical analysis of the HF process with a modular polymeric die. The axisymmetric case study with undercuts also allowed the evaluation of the process's applicability to more complex geometries. The numerical model was finally validated by comparing the results with data from experimental tests.

Material and methodology

Material. The chemical composition (weight%) and the main mechanical properties of the investigated alloy (AA5754-H111) are presented in Table 1; in addition, the mechanical and deformation behaviour are summarized by the curves in Fig. 1 which were obtained by tensile and formability tests, respectively.

Table 1 – Chemical composition % and mechanical properties of the investigated alloy.

Mn	Fe	Mg	Si	Cr	Cu	Mn + Cr	Ti	Others	Zn	Al
≤0.5	≤0.4	1.6-3.6	≤0.4	≤0.3	≤0.1	0.1-0.6	≤0.2	≤0.15	≤0.2	Balance
Proof Stress		Tensile Strength			Hardness Brinell		Elongation A50 mm			
60 Min MPa		160 - 200 MPa			44 HB		12 Min %			

Case study. The case study was an axial symmetric part but with undercuts which present a challenge for the forming process (Fig. 2). While axial symmetry simplifies the analysis, the undercuts require careful control of the deformation process to ensure optimal material flow and prevent defects. For its fabrication, circular samples (80 mm in diameter) with a thickness of 0.5 mm, all taken from the same sheet, were adopted for the experimental activities.

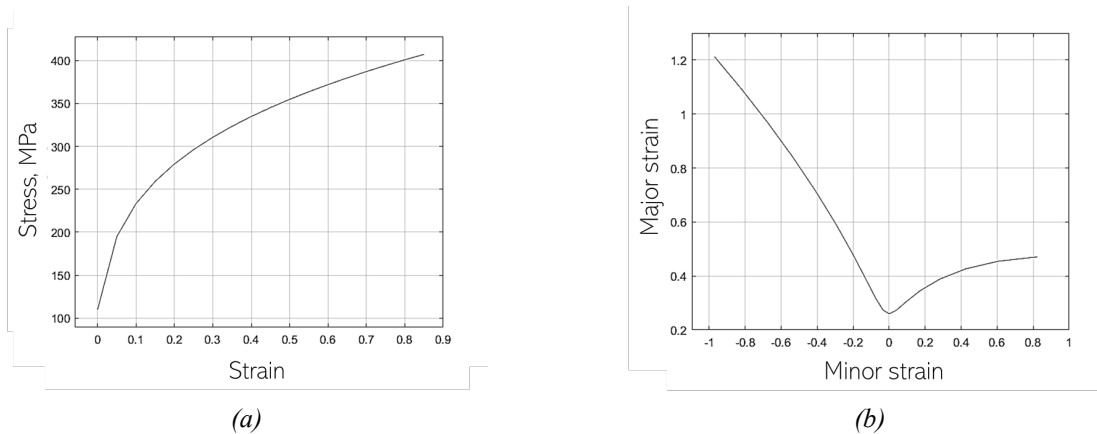


Figure 1 – Flow stress curve (a) and FLC (b) for the investigated alloy.

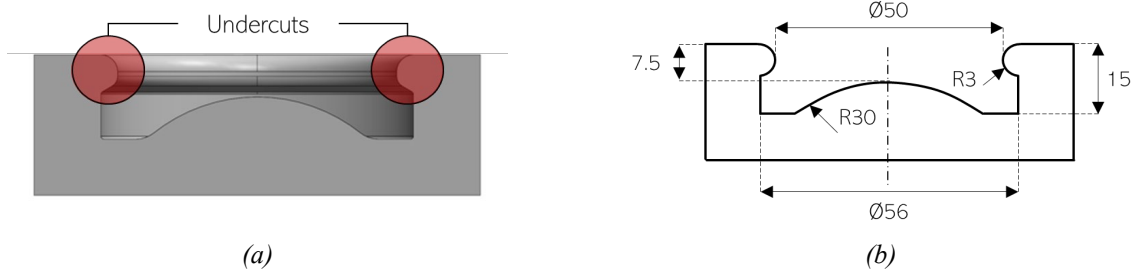


Figure 2 – Schematic (a) and dimensions in mm (b) of the case study.

The die sizing (and consequently the component itself) was determined through a FE based approach.

Numerical analysis

The numerical simulations were conducted using the commercial software ABAQUS®. In particular, the numerical model was created using two successive design steps: the first one was focused on the development of a sufficiently simplified model to identify (i) a final geometry of the case study, (ii) its dimensions, and (iii) to evaluate the initial sheet metal diameter to be used in the subsequent experimental validation tests; in the second step the model's complexity was increased by introducing some previously omitted aspects, like the material properties of the polymeric die.

The simulations performed in the first step allowed to assess of the component dimensions, which also helped determine the size of the modular die to be created using AM technology, as well as to design all the components of the equipment used in the experimental validation phase. For these simulations a 2D axisymmetric model was adopted, considering all parts of the die as rigid body, while the sheet metal was modelled as a deformable body. The friction coefficient between the parts was set equal to 0.2. Interactions were defined between the upper surface of the sheet and the blankholder, as well as between the lower surface of the sheet and the die. Both the die and the blankholder were pinned. The sheet metal, with an initial thickness of 0.5 mm, is positioned in such a way that there was no initial interaction with the blankholder, allowing the oil to act on the entire surface of the sheet. The pressure was linearly increased up to 700 bar (the maximum value experimentally available). The sheet metal was modelled as a wireframe, allowing for further reduction in computational costs. Fig. 3 shows the outline of the model adopted in this first step.

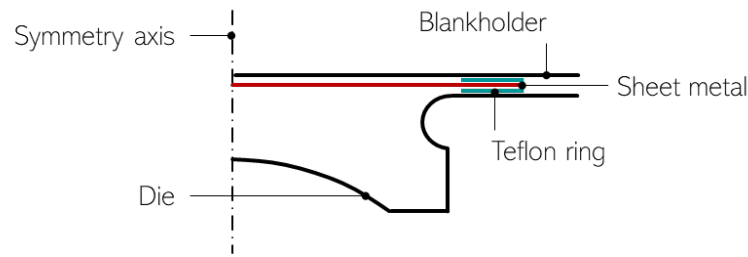


Figure 3 – Schematic of the numerical model.

Subsequently, in the second step of the numerical activities, all deformable bodies were modelled as “shell” while the blankholder was modelled as “wire”. Furthermore, in this case, the issue of die disassembly was evaluated through two distinct strategies, as summarized in Fig. 4: the polymeric material parts are identified by numbers 1 to 3, depending on the strategy. In contrast, part 4 represents the metal cavity into which the modular die is inserted.

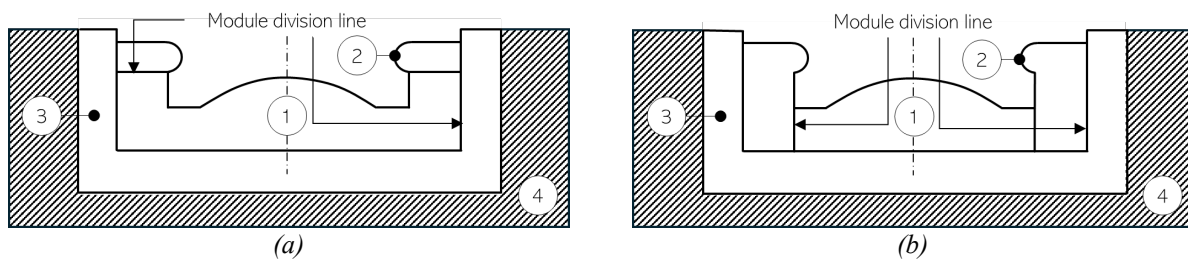


Figure 4 – Schematic of the die division strategy (a) First and (b) Second strategy.

In addition, the adoption of a Teflon ring was considered for both sealing and reducing friction of the sheet metal. For this reason, the ring was modelled, and its mechanical properties were assigned, managing it as a purely elastic body: (i) density equal to 2200 kg/m³, (ii) Young’s modulus of 750 MPa and the (iii) Poisson’s ratio fixed at 0.4.

Regarding the modelling of the load acting on the sheet metal, the oil pressure on the upper surface of the sheet metal was included in the model. The presence of the Teflon ring on the sheet metal limits the area on which this pressure acts; in this case a ring with an inner diameter of 56 mm and an outer diameter of 80 mm (thick 1 mm) was used. As the part of the sheet metal initially under the Teflon ring slides, it is subjected to the action of the oil. To simulate this phenomenon, the VDLOAD subroutine was used; this method allows variable loads to be simulated depending on position and time.

Table 2 reports the main properties of the polymeric material (Onyx) used in this work [36].

Table 2 – Properties of the adopted ONYX for the deformable die.

Density	Tensile Strength	Young’s modulus	Poisson’s Ratio
1.2 g/cm ³	40 MPa	2.4 GPa	0.43

The die was modelled as a purely elastic body. As shown in Fig. 4, it is composed by 3 parts, all modelled as purely elastic deformable bodies. In addition, the die was inserted into a steel case (elastic modulus: 210 GPa; Poisson’s ratio: 0.33). The friction coefficient between the sheet metal and the Teflon ring was set, after a preliminary calibration stage, equal to 0.025, while that for all other interactions is 0.2 (according to the preliminary analyses). In this phase, constraints were applied to the modelled bodies: for the blankholder, only vertical movements were allowed, while the radial and rotation displacements were blocked. The polymeric die was completely free, just like the sheet metal, while the steel case (body 4 in Fig. 4) had no possibility to move.

The preliminary simulations using the simplified model were conducted setting the dynamic implicit solver, while the simulations using the more refined model adopted the dynamic explicit

method due to several contact issues between the deformable bodies. However, mass scaling was used to reduce the computation time.

Polymer die manufacturing

All the parts composing the modular dies were produced by Material Extrusion with Mark Two (Markforged™). Their modularity is assessed to evaluate if a single portion of the die can be easily replaced. Onyx filament (Nylon + carbon, Markforged™.) is extruded at 270 degrees Celsius with a nozzle of 0.2mm. The layering of the parts has been maintained at high precision to 0.1mm with a whole solid fill strategy (Fig. 5).

The final design consisting in die samples composed by one base and one couple of half rings (second strategy) lasted approximately 31 hours with a total material volume of 190 cm³.



Figure 5 – Printing plate composed by two replica of the polymer dies with a 3D detail on the support material filling (in purple).

Experimental validation

Numerical results were validated through experimental tests and using a specifically designed equipment. The presence of the undercut justified the use of a polymeric modular die, allowing the component to be removed at the end of the forming cycle, as well as leveraging the flexibility of AM technologies for its production. To withstand the high stresses involved in the HF process, the die parts were made from Onyx, a polymer composed of a nylon matrix reinforced with carbon fibers (Table 2).

The HF tool was assembled on a 30 tons electro-hydraulic press machine. The simple architecture of the system was appropriately used for positioning the polymeric die inside a tool made of 40NiCrMo7 steel, as well as for the implementation of a plate that served as blankholder. More details are given in Fig. 6.

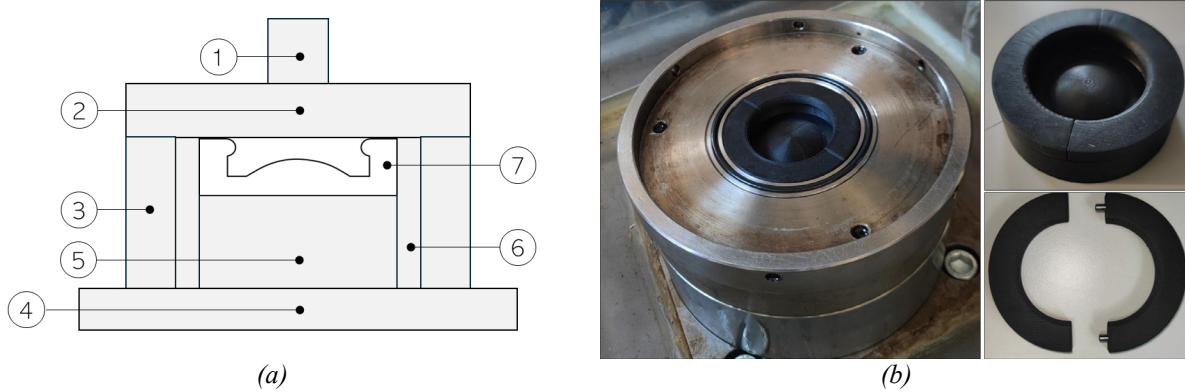


Figure 6 – (a) Complete tooling scheme: Interface punch-equipment (1), Pressing plate (2), Metal ring (3), Interface Base press-facility (4), Height regulator (5), Circular metal plate (6) and Polymeric die (7). (b) Experimental facility.

Mineral oil was pressurized by a hydraulic power unit up to the maximum pressure of 700 bar; a HAWE D74851 proportional pressure relief valve managed by LABVIEW was used to define the pressure profile; a load cell was used to measure the blankholder force during the tests.

Results and Discussion

Numerical analysis. Four starting geometries, all of which have at least one undercut, were identified (Fig. 7). To analyse the feasibility of the geometry via HF process, the FLDCRT (calculated by comparing the major deformation of any node with the maximum deformation of the FLC at the same minor deformation) was considered as an output variable (Table 3)

Table 3 – FLDCRT values for the four investigated geometries.

a	b	c	d
1.374	1.021	0.855	0.809

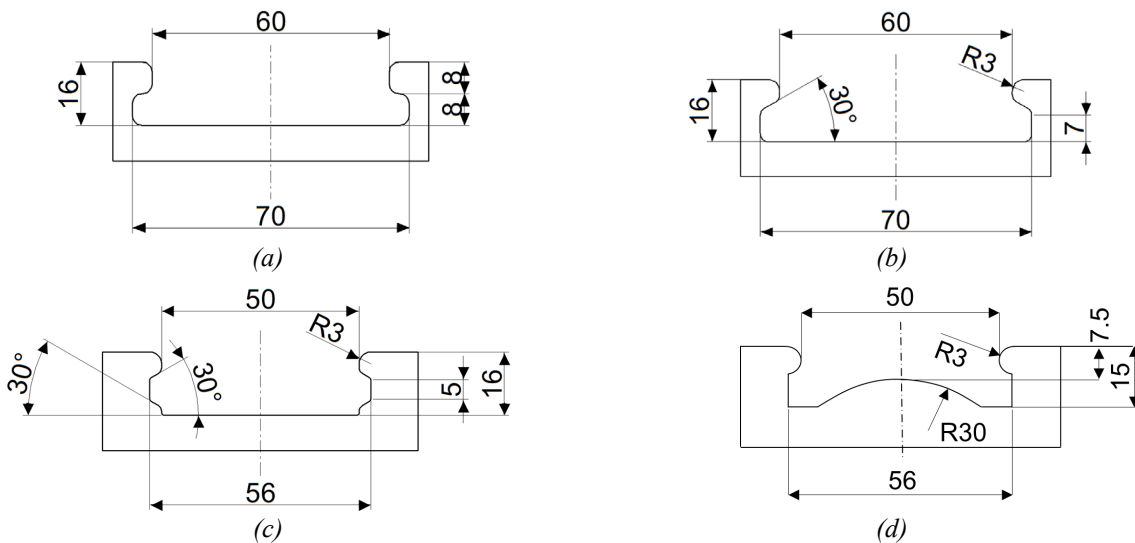


Figure 7 – Geometries selected for the preliminary analysis.

It can be noted that for the first two geometries the maximum calculated values are greater than 1, thus suggesting that there are areas of the sheet metal where the deformation path exceeds the formability limits. Based on these results, the geometry “d” was chosen as case study to be experimentally validated; the main dimensions are reported in Fig. 2b.

In addition, three different sizes of the initial sheet diameter (80, 84 and 90 mm) were considered to determine which was the best choice in terms of die cavity filling. Fig. 8a shows the

trend of the sheet displacement (monitored in the black point) as a function of the initial blank diameter.

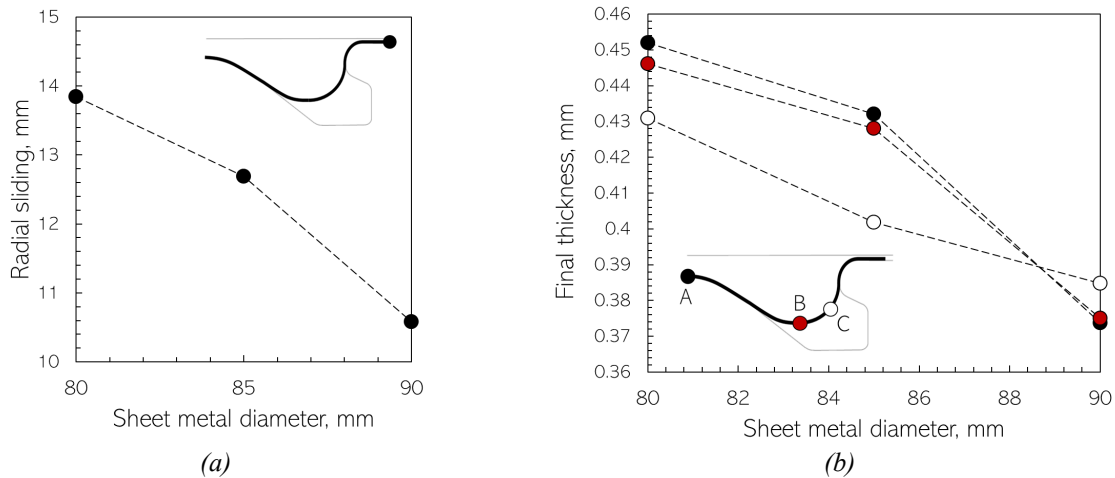


Figure 8 – Sheet displacement in accordance with the undeformed sheet diameter.

As the diameter decreases, the displacement increases. Such a trend is due to the larger interaction surface between the sheet and the die: in fact, when pressure acts on the surface, a force is generated that limits the displacement and, consequently, the complete filling of the die.

In Fig. 8b thicknesses are plotted as a function of the initial sheet diameter using the shell model. It can be observed that as the initial diameter increases, the final component undergoes greater thinning. Additionally, the area that will experience the greatest thinning is placed in correspondence of the point C.

To summarize, the numerical analyses aimed at determining the optimal initial diameter of the undeformed sheet highlighted that using a diameter of 80 mm would result in greater displacement and better die filling. Furthermore, this solution would allow for a more uniform thickness distribution in the final component.

Since numerical analyses modelling the polymeric die were conducted using the dynamic explicit solver, the kinetic energy of the modelled system (ALLKE) was compared to the total internal energy of the system (ALLIE) in order to check if it is negligible, thus avoiding affecting the deformation of the material since the HF is a quasi-static process.

The adoption of the first division strategy presented several critical issues. As shown in Fig. 9a, the upper ring undergoes significant deformations, shifting from its original position and bending inward. This movement could lead to oil leakage beneath the spacer. Although such leakages are not visible because the presence of oil in the chamber was not modelled, they could cause counter pressures that prevent the complete forming of the sheet. Additionally, the bending of the upper ring could result in a final geometry that does not match the desired shape. This second strategy allows the upper part of the die to be stiffer; in fact, as can be seen from Fig. 9b, the deformation was considerably lower than that obtained in the previous case.

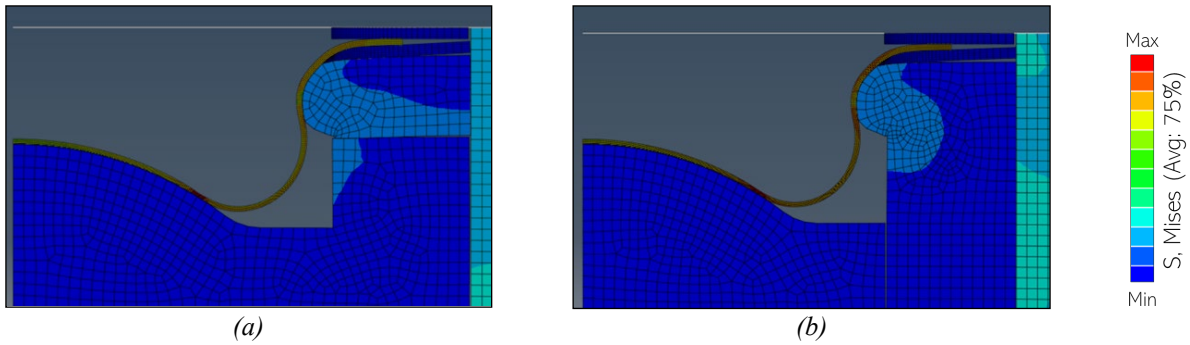


Figure 9 – Deformation obtained from the numerical model at 200 bars with the first (a) and the second (b) strategies.

The simulations shown in Fig. 9 were conducted setting the maximum pressure to 200 bar; in fact, at a pressure of 250 bar (Fig. 10) an evident thinning of the sheet metal was obtained in the area circled in red, thus revealing the occurrence of rupture.

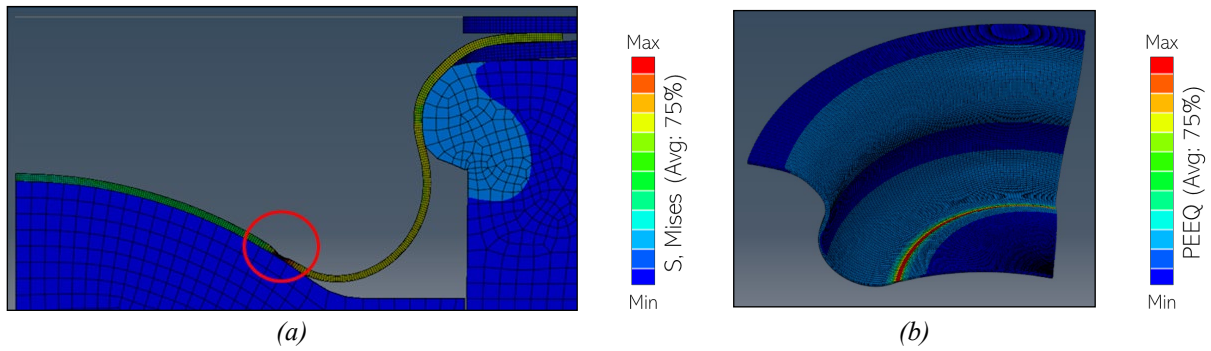


Figure 10 – Analyses for the second strategy at 250 bars: (a) Deformation and (b) PEEQ.

Experimental validation

The first test specimen, which can be observed in Fig. 11, was obtained at a pressure of 200 bar. Three replications were performed. To validate the numerical model, several parameters were analysed, such as the external diameter of the flanged area (to assess the material drawing during deformation), the height of the component and its final thickness distribution measured in the radial direction (after cutting the part).

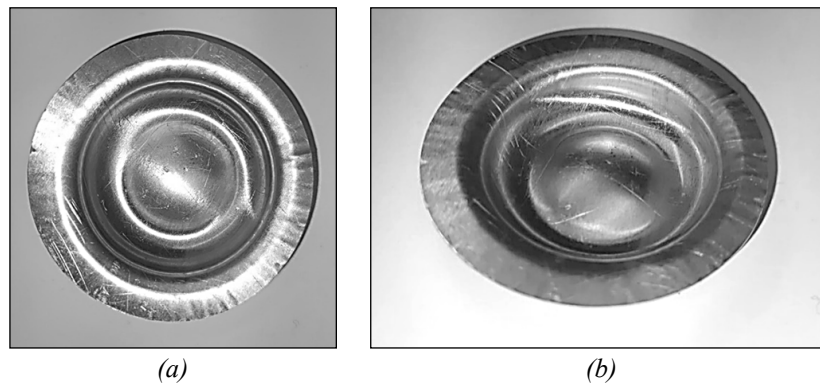


Figure 11 – Deformed sample obtained with a maximum pressure of 200 bar.

The measured external diameter of the part shown in Fig. 11 was 72 mm, which means that, starting from a sheet with an initial diameter of 80 mm, the displacement was 4 mm with respect to the radius. From the numerical simulation, a displacement of 5.3 mm was measured, thus indicating that, under the same conditions, the numerical model deviated by 20% from the

experimental condition. In terms of final height of the component, the sample obtained in the experimental tests reached a final measured height of 13.8 mm, while the simulated value was 14.4 mm. Once again, it can be stated that the numerical model is reasonably predictive of the experimental tests, with an error of 5% in the results.

After cutting the part along the diameter, the thickness at various points was measured and compared with the numerically predicted values in the same points along the radial profile (considered points are in Fig. 8b); acquired data and the correspondent numerical ones are reported in Table 4.

Table 4 – Numerical/Experimental comparison of thicknesses, measured at the three identified points.

	A	B	C
Experimental	0.44	0.42	0.54
Numerical	0.43	0.40	0.53

It can be noted that the sheet experienced a thinning in the central area (A) and a thickening in the flange area (C). As reported in Table 4, numerical results deviated by a maximum of 5% from the experimental data, thus confirming the robustness of the FE simulations.

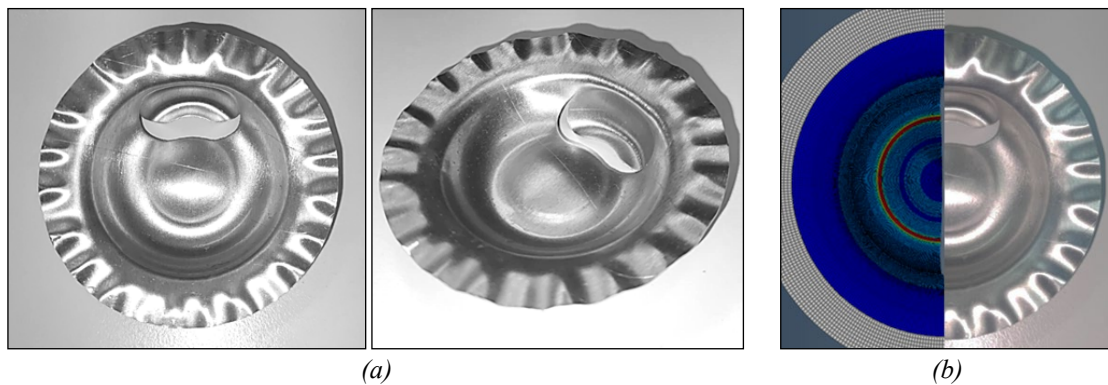


Figure 12 – Deformed sample (up to rupture) obtained with a maximum pressure of 250 bar (a); Numerical/Experimental comparison of the rupture zone (b).

Even in terms of failure prediction, the FE simulation resulted to be in agreement with the experiments: in fact, at a pressure of 250 bar the sample fractured (see Fig. 12a) and the numerical simulation, at the same pressure, predicted an evident thinning in the same region.

Fig. 12b directly compares the numerical and the experimental results: on the left there is the deformed configuration predicted by the FE simulation at 250 bar, in which the thinning zone is visible (red area), while on the right is the test specimen which fractured at the same level of pressure. It can be seen how the failure zone of the test specimen fits with the one predicted by simulation.

Conclusions

This study evaluated, through a numerical/experimental approach, the potential of using modular polymeric dies made via AM for the fabrication of complex shaped components with undercuts using the HF process at room temperature. The results obtained are promising, since the part was successfully produced using an Onyx tool assembled into a steel case. The FE simulations revealed to play a key role for both the proper design of the process and the substantial reduction of overall time and costs. In addition, the FE approach allowed to define the correct strategy of splitting the polymeric die, being such a phase crucial for achieving compliant and sound parts.

Experimental and numerical results obtained in the present work, which showed a good fitting, revealed that the proposed approach for producing complex shaped parts with undercuts, based on the adoption of the HF process at room temperature using customizable and modular polymeric

dies made by AM, is feasible and effective. Therefore, further advanced research is needed for optimizing process parameters and for integrating the approach into established industrial processes.

Acknowledgements

This work was financed by the European Union – NextGenerationEU (National Sustainable Mobility Center CN00000023, Italian Ministry of University and Research Decree n.1033 - 17/06/2022, Spoke 11 - Innovative Materials & Lightweighting). The opinions expressed are those of the authors only and should not be considered as representative of the European Union or the European Commission's official position. Neither the European Union nor the European Commission can be held responsible for them.

Specifically, the activities carried out fall within the scope of the project "PROduction by 3D printing of modular tools for Highly customizable hydroforming of sheet metals (PROHYDRO)" funded by means of the Closed "Call for PoC" of the National Sustainable Mobility Center.

References

- [1] J.C. Kelly, J.L. Sullivan, A. Burnham, A. Elgowainy, Impacts of Vehicle Weight Reduction via Material Substitution on Life-Cycle Greenhouse Gas Emissions, *Environ Sci Technol* 49 (2015) 12535–12542. <https://doi.org/10.1021/acs.est.5b03192>
- [2] F. Czerwinski, Current trends in automotive lightweighting strategies and materials, *Materials* 14 (2021). <https://doi.org/10.3390/ma14216631>
- [3] M. Türköz, Ö.N. Cora, H. Gedikli, M. Dilmeç, H.S. Halkacı, M. Koç, Numerical optimization of warm hydromechanical deep drawing process parameters and its experimental verification, *J Manuf Process* 57 (2020) 344–353. <https://doi.org/10.1016/j.jmapro.2020.06.020>
- [4] P. Moriarty, D. Honnery, The prospects for global green car mobility, *J Clean Prod* 16 (2008) 1717–1726. <https://doi.org/10.1016/j.jclepro.2007.10.025>
- [5] C. Bell, J. Corney, N. Zuelli, D. Savings, A state of the art review of hydroforming technology: Its applications, research areas, history, and future in manufacturing, *International Journal of Material Forming* 13 (2020) 789–828. <https://doi.org/10.1007/s12289-019-01507-1>
- [6] P. Ottosson, E.L. Westman, I. Nygren, T. Pettersson, F. Niklasson, L.E. Brattström, Design of a sustainable Flexforming procedure for aero engine components in alloy 718, *ICAS Proceedings* (2024) 1–13.